Exp. Theo. NANOTECHNOLOGY 9 (2025) 563-569 https://doi.org/10.56053/9.4.563

$AgZnFe_2O_3$ quaternary alloy: Synthesis, analysis and characterization for potential antibacterial application

Asaad T. Al-Douri[1], Alaa A. Khaleel[2], Luay Mannaa ibrahim[1], Abeer Talib Abdulqader[1], Ammr Khalid Shihab[3], Mustafa Khaleel Ibrahim[1], Maksood Adil Mahmoud Al-Doori[1]*

[1]College of Health & Medical Techniques–Al-Dour, Northern Technical University, Iraq
[2]Department of Biology,College of Science, Tikrit University, 34001 - Iraq
[3]Al-Dour Technical Institute, Northern Technical University, Iraq
[*]) Email: asta7062@gmail.com

Received 15/5/2025, *Received in revised form* 11/9/2025, *Accepted* 27/9/2025, *Published* 15/10/2025

The $AgZnFe_2O_3$ quaternary alloy nanostructure is successfully synthesized using a cost-effective and environmentally friendly chemical co-precipitation method. The morphology is investigated by scanning electron microscopy (SEM), which revealed uniformly distributed nanograins with an average grain size of 52.02 nm. Optical properties are examined using UV-visible spectrophotometry (UV-vis) and Fourier-transform infrared spectroscopy (FTIR). The bandgap energy is determined to be 3.15 eV, while the absorption spectra indicate minimal absorption, suggesting higher transmission and reflection. Empirical models are applied to validate the dielectric constant and refractive index, with the Ghosh et al. model found to be the most suitable. FTIR analysis confirms weak absorption bands and characteristic stretching vibrations, further supporting the material's structural stability. Importantly, the synthesized $AgZnFe_2O_3$ nanostructure demonstrates promising antibacterial potential against antimicrobial-resistant Gram-negative pathogens, highlighting its suitability for biomedical and therapeutic applications.

Keywords: $AgZnFe_2O_3$; SEM; UV; FTIR.

1. INTRODUCTION

The use of nanostructures has emerged as an attractive strategy for managing or preventing different infections. For this reason, the aim of the present work is to reduce the widespread and inappropriate use of antimicrobial therapeutic agents due to their high occurrence and challenges associated with treating bacteria resistant to multiple drugs [1]. The bacteria exhibit a noteworthy array of virulence factors capable of influencing a diverse range of host cell processes [2]. The widespread utilization of antibiotics

has played a role in their substantial prevalence in the environment. This has favored the development of resistant microorganisms through processes such as selection, mutation, and horizontal transfers via recombination [3].

Nanostructures with antibacterial properties are believed to have the potential to reduce or prevent the emergence of resistant bacteria by targeting multiple biomolecules simultaneously, thereby hindering the development of resistant strains [4]. Due to their high surface-to-volume ratio, nanostructures can effectively interact with clinically significant bacteria, making them promising antibacterial agents. Additionally, they enhance the ability to eliminate microbial pathogens that have developed resistance to conventional antimicrobials. Research suggests that Gram-positive bacteria exhibit greater resistance to the antibacterial mechanisms of nanoparticles (NPs), likely due to differences in cell wall composition [5]. In contrast, Gram-negative bacteria, such as E. coli, possess an outer layer of lipopolysaccharides, 1–3 μm thick and a peptidoglycan layer, ~ 8 nm thick, which may facilitate the penetration of ions released from NPs into the bacterial cell. Currently, environmentally friendly green synthesis methods are employed to produce various nanoparticles, including silver-based NPs, zinc oxide (ZnO) NPs and titanium oxide (TiO_2) NPs, all of which exhibit antibacterial activity against a broad spectrum of microorganisms [6,7]. Moreover, several studies have demonstrated that magnesium oxide (MgO) nanoparticles can be successfully synthesized using biological substrates through green synthesis, resulting in eco-friendly products that are safe for the environment. Additionally, the combination of plant extracts with nanoparticles helps to reduce the risk of cytotoxicity [8]. It is indicated that toxicity assessments in animals and cell lines have suggested that green-synthesized magnesium nanoparticles are not toxic [9]. Furthermore, research by Abinaya et al. [10] has demonstrated that magnesium oxide nanoparticles exhibit antioxidant activity, are non-toxic, and possess excellent stability, making them highly suitable for nanoscale production. Magnesium-based nanoparticles (NPAg) present a promising alternative to heavy metal-based nanoparticles, as they can be efficiently metabolized and degraded within the body. In cases of normal kidney function, the degradation products, including Ag^{2+} and OH^{-} ions, can be effectively excreted, thereby preventing excessive metal accumulation. Additionally, NPAg has the capability to generate reactive oxygen species (ROS), which induce oxidative stress in both in vitro and in vivo cell cultures, leading to strong anti-pathogenic effects [11].

This work aims to synthesize and investigate the $AgZnFe_2O_3$ quaternary alloy nanostructure using the chemical co-precipitation method, chosen for its simplicity, cost-effectiveness, and environmental sustainability. The study seeks to highlight the morphological and optical properties of the prepared nanostructure through SEM, UV-Vis, and FTIR analyses. A central goal of this research is to bridge the gap in the literature regarding $AgZnFe_2O_3$ quaternary nanostructures, which have not been widely reported.The primary objective is to explore the correlation between nano-structural features and optical behavior, thereby opening pathways for potential applications, particularly in antibacterial fields. This research also aims to examine the influence of the synthesis route on the homogeneity, grain packing, and optical response of the $AgZnFe_2O_3$ nanostructure.

2. EXPERIMENTAL

In this work, it is provided a concise explanation of the synthesis employed for creating a quaternary alloy of AgZnFe2O3 along with an overview of the primary techniques utilized for its characterization. The synthesis of AgZnFe2O3 has involved a chemical co-designation approach, where the solution is consistently agitated and then cooled to ambient temperature. The outcome of this process is the production of AgZnFe2O3 quaternary alloy, and the procedural details are as follows:
Start by dissolving 1 g of dried Gujarat, an herbaceous plant with a soft, green, delicate stem lacking woody tissues, in 100 ml of distilled water for 30 minutes. Meanwhile, dissolve zinc nitrate (molecular weight: 189.39) in distilled water at 60 °C for 30 minutes [12]. The two solutions are then combined and stirred using an agitator for 30 minutes to synthesize the nanoparticles (NPs).

In the second step, dissolve another 1 g of dried Gujarat in 100 ml of distilled water for 30 minutes. Next, dissolve iron nitrate (molecular weight: 24.86) in distilled water at 60 °C for 30 minutes [13]. Finally, mix both solutions using an agitator for 30 minutes to obtain the NPs.

Dissolve magnesium nitrate and mix it with the dissolved Gujarat plant to induce thawing and the formation of NPs. Ultimately, integrate these final three solutions into the processes outlined in the initial two steps to synthesize the quaternary alloy nanoparticles, specifically AgZnFe2O3. For structural analysis, the surface morphology, shape, and grain size of $AgZnFe_2O_3$ quaternary alloy nanoparticles are examined using a scanning electron microscope (SEM JSM-6010LV, USA). Optical properties at ambient temperature are assessed through UV-visible spectrophotometry (UV-vis) using a Perkin Elmer Lambda 950 instrument, USA.

The composition and quality of AgZnFe2O3 quaternary alloy nanoparticles are investigated using Fourier transformation infrared spectroscopy (FTIR) within the 4000-500 cm-1 region (PerkinElmer NIRFlex N-500 instrument, Switzerland).

3. RESULTS AND DISCUSSION

The morphology of $AgZnFe_2O_3$ exhibits agglomerated, flower-like grains. As shown in Figure 1, the agglomerated nanoparticles (NPs) adhere well to the surface due to the material composition, highlighting a noticeable similarity. Structural analysis of $AgZnFe_2O_3$ quaternary alloy nanoparticles confirms good crystallinity. The SEM image further reveals the homogeneity of the flower-like NPs (Figure 1).

For the $NiZnFe_2O_3$ quaternary alloy nanostructure, dense crystallite formation is evident. Figure 1 illustrates that the agglomerated nanoparticles and well-formed nanostructures adhere to the surface due to the material composition, showing a noticeable similarity. The homogeneity of the cube-like nanostructure in the $NiZnFe_2O_3$ image corresponds to the crystallite size. The measured grain sizes are listed in Table 1.

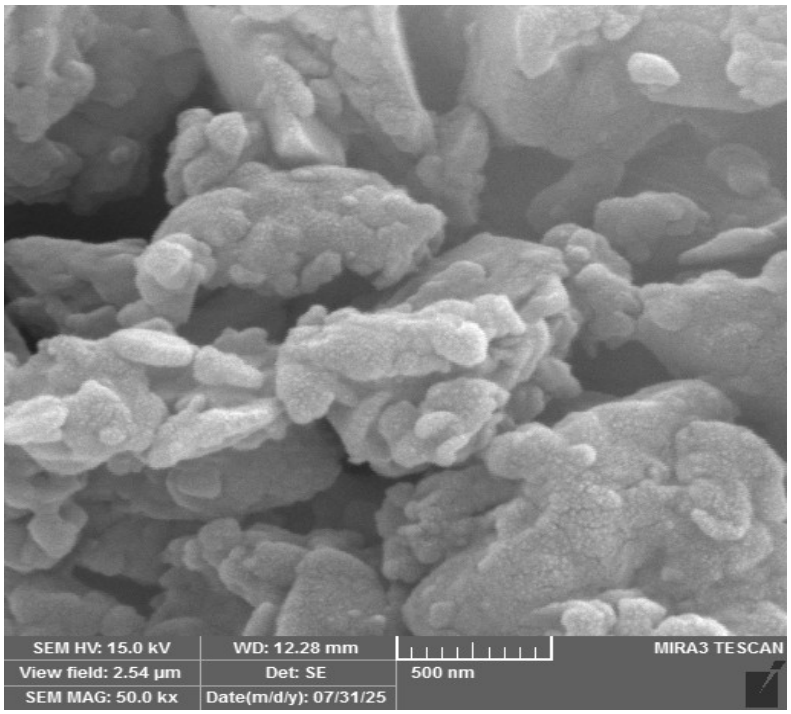

Figure 1 SEM image of AgZnFe2O3 alloy nanostructure.

Table 1 Grain size, bandgap corresponding to refractive index, and optical dielectric constant of AgZnFe2O3 quaternary alloy nanostructure.

Alloy	**Grain size (nm)**	E_g **(eV)**	***n***	ε_∞
$AgZnFe_2O_3$	52.02	2.15	2.40^a 2.50^b 2.45^c	6.15^a 6.30^b 6.15^c

Ref. [14]; Ref. [15]; Ref. [16].

Optical studies are conducted to examine absorption, transmission, reflection, absorption coefficient and FTIR from an analytical viewpoint. The gains of AgZnFe2O3 quaternary alloy nanostructure are agglomerated and have a nano-scale as illustrated in Figure 1 and presented in Table 1.

Absorption spectra of tetragonal $AgZnFe_2O_3$ alloys are recorded at room temperature using UV-vis spectroscopy, covering a wavelength range of 350–1150 nm, as shown in Figure 2. These spectra reflect the characteristic behavior of the material. An inverse relationship is observed between absorbance and atomic number. Similarly, the transmittance of $AgZnFe_2O_3$ exhibits an inverse relationship with absorbance, while transmittance and wavelength share a direct relationship. The lowest transmittance is approximately 90% (Figure 2).

The absorption coefficient shows high values at shorter wavelengths and gradually decreases with increasing wavelength within the energy gap (Eg) range between 350 - 390 nm, as shown in Figure 3. This indicates that the absorption of photons is primarily direct, while the absorption spectrum includes

both direct and indirect absorption mechanisms, arising from differences in the crystal structure corresponding to different atomic numbers [17-19].

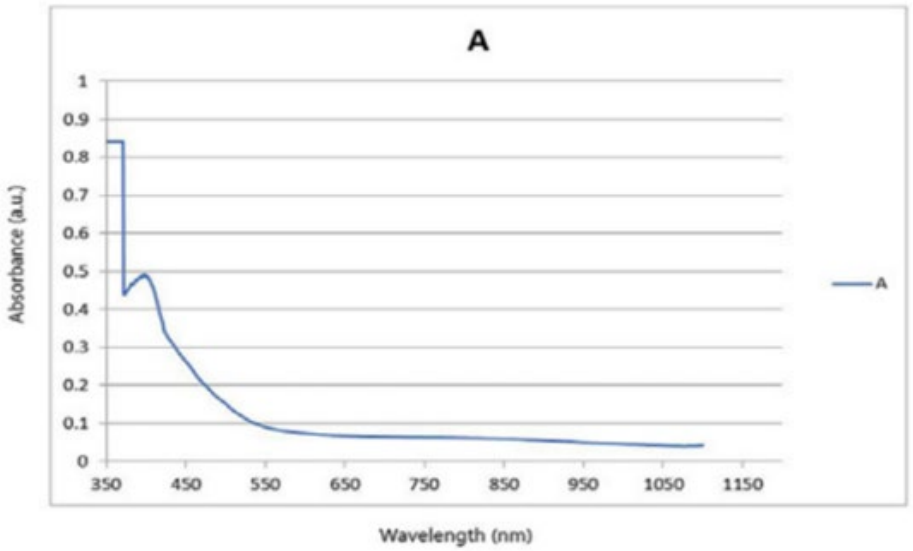

Figure 2 Absorbance AgZnFe2O3 quaternary alloy nanostructure.

Fourier transform infrared (FTIR) Figure (4) illustrates the FTIR spectrum of the $AgZnFe_2O_3$ nanocomposite. A broad absorption band observed at 3421 cm^{-1} corresponds to O–H stretching vibrations, which may be attributed to surface hydroxyl groups or adsorbed moisture. The weak bands at 2931–2875 cm^{-1} are assigned to C–H stretching vibrations. The absorptions appearing in the region of 1849–1639 cm^{-1} can be related to C=O and C=C stretching, indicating the possible presence of residual organic species on the nanoparticle surface. Peaks at 1549–1440 cm^{-1} are associated with C=C and N–O stretching vibrations.

The bands in the range of 1236–1043 cm^{-1} are ascribed to M–O–M stretching modes (M = Fe, Zn, Ag), confirming the formation of metal–oxygen bonds within the nanocomposite structure. Characteristic absorptions at 923–856 cm^{-1} further support the crystalline nature of the metal oxide phases. Importantly, the strong peaks between 623–427 cm^{-1} are attributed to Fe–O and Zn–O stretching vibrations, which provide direct evidence for the successful formation of Fe_2O_3 and ZnO phases in the $AgZnsFe_2O_3$ nanocomposite [20].

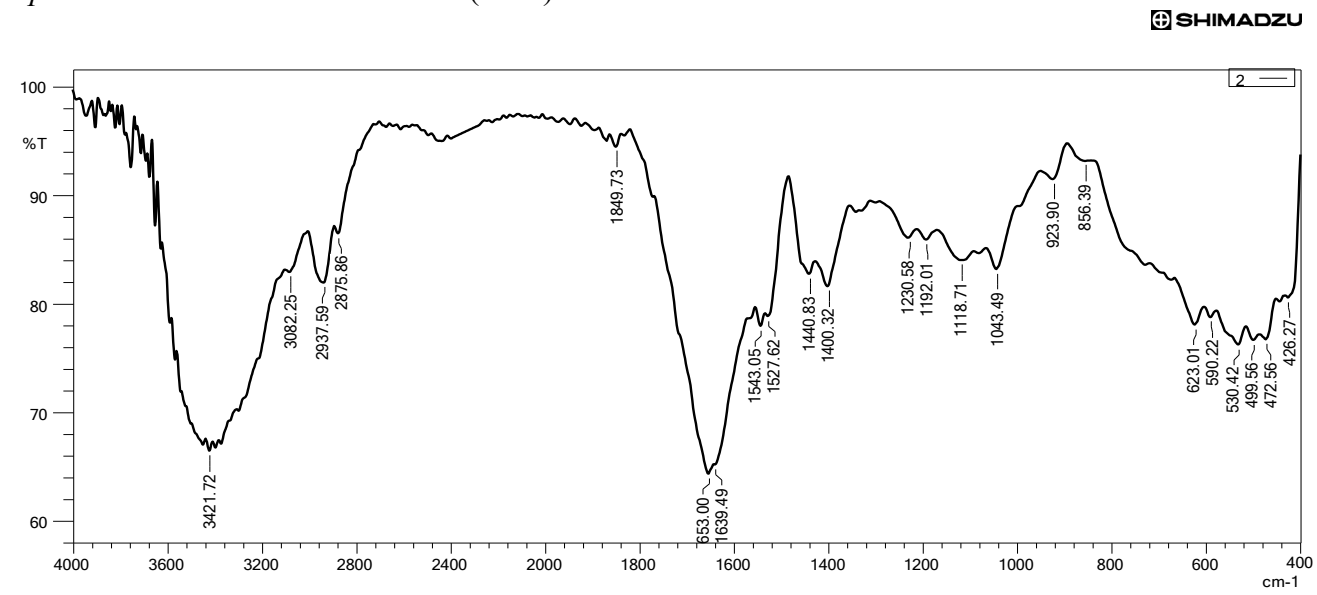

1

Figure 3 FTIR of AgZnFe2O3 quaternary alloy nanostructure in the range, 400 to 4000 cm-1, which corresponds to stretching vibrations.

4. CONCLUSIONS

This study also finds that the $AgZnFe_2O_3$ quaternary alloy nanostructure inhibits the growth of harmful antimicrobial-resistant Gram-negative pathogens, supporting its potential as an antibacterial agent with numerous biomedical and therapeutic applications. The $NiZnFe_2O_3$ quaternary alloy nanostructure is prepared using the chemical co-precipitation method. Notably, the results indicate improved morphological characteristics, with homogeneously formed nanograins. The grain size is measured at 52.02 nm, and the band gap is found to be 3.15 eV. The absorption spectra are the lowest, suggesting that transmission and reflection are at their highest. The Ghosh et al. model is proposed for potential antibacterial applications. FTIR analysis shows clusters with a mean size and the weak absorption, very weak vibrations, and medium-strong stretching vibrations, further validating the suitability of the $AgZnFe_2O_3$ quaternary alloy nanostructure for its intended applications.

References

[1] D.S. Lee, S.J. Lee, H.S. Choe, Biomed. Res. Int. 55 (2018) 7656752
[2] P. Shakya, D. Shrestha, E. Maharjan, V.K. Sharma, R. Paudyal, Open Microbiol J. 11 (2017) 30
[3] Magdalena Męcik, Martyna ButaHubeny, Łukasz Paukszto, Mateusz Maździarz, Journal of Environmental Management 348 (2023) 119303
[4] H. Sellami, S.A. Khan, I. Ahmad, A.A. Alarfaj, A.H. Hirad, A.E. Al-Sabri, Int. J. Mol. Sci. 22 (2021) 12562
[5] A. Mobeen, C.M. Magdalane, S.K. Jasmine Shahina, D. Lakshmi, D. A. Ramalingam, Raja, Surf. Interfaces 17 (2019) 100381
[6] Atef S. El-Gebaly, Ahmed R. Sofy, Ahmed A. Hmed, Ahmed M. Youssef, Biocatalysis and Agricultural Biotechnology 55 (2024) 103006

[7] S. Shaikh, S.M.D. Rizvi, S. Shakil, T. Hussain, T.M. Alshammari, W. Ahmad. J. Cell Biochem. 118 (2017) 2808
[8] M. Maghimaa , Suresh Sagadevan, Punna Rao Suryadevara, Hari Hara Sudhan, Gowri Sankara Rao Burle, Janne Ruokolainen, Vinod Kumar Nelson, Kavindra Kumar Kesari, Inorganic Chemistry Communications 173 (2025) 113806
[9] Inas Y.Younis, Seham S. El Hawary, Omayma A. Eldahshan, Marwa M.Abdel Aziz, Zeinab Y. Ali, Scientific Reports 11 (2021) 16868
[10] S. Abinaya, Helen P. Kavitha, M. Prakash, A. Muthukrishnaraj. Sustainable chemistry and Pharmacy 19 (2021) 100368
[11] G.A. Kumar, H.S.B. Naik, R. Viswanath, G. Krishnamurthy, P. Walmik, Emergent Mater. 3 (2020) 946
[12] A.S. Ibraheam, Y. Al-Douri, U. Hashim, M.R. Ghezzar, A. Addou, W.K. Ahmed, Sol. Energy 114 (2015) 50
[13] M. Pilvet, M. Kauk-Kuusik, M. Altosaar, M. Grossberg, M. Danilson, Thin Solid Films 582 (2015) 183
[14] N. M. Ravindra, S. Auluck, V. K. Srivastava, physica status solidi (b) 93 (1979) k160
[15] P. J. L. Herve, L. K. J. Vandamme, Journal of Applied Physics 77 (1995) 5488
[16] D. K. Ghosh, L. K. Samanta, G. C. Bhar, Infrared Physics 24 (1984) 58
[17] Maksood Adil Mahmoud Al-Doori1, Asaad T. Al-Douri1, Nahedh Ayad Faris, Exp. Theo. NANOTECHNOLOGY 9 (2025) 503
[18] Ahmed Suhail Hussein, Noor Khalid Ismael, Asaad T. Al-Douri, Abbas Saeb Zaham, Ali Y.Alwan, Mais Qasem Mohammed, Sama Amer Abbas El-Tekreti, Shaimaa Tarik Mahmood, Saeb Jasim Mohammed Alnajm,Younis W. Younis, Maksood Adil Mahmoud Al-Doori. Exp. Theo. NANOTECHNOLOGY 9 (2025) 512
[19] Safa Salah Salman, Asaad T. Al-Douri, Albosale Abbas Hadi, Saeb Jasim Mohammed Alnajm, Exp. Theo. NANOTECHNOLOGY 9 (2025) 372
[20] Yan Wang, Xiang Gao, Wenzhi Zhang, Chunyan Luo, Lijuan Zhang, Pu Xue, Journal of Alloys and Compounds 757 (2018) 381